

dispersions were applied to all atoms.

Acknowledgment. We thank the National Science Foundation (Grant CHE-894209) for support, Johnson Matthey, Inc., for a loan of gold salts, Marilyn M. Olmstead for assistance with the crystallography, and C. LeMaster for assistance with the NMR

spectral simulations.

Supplementary Material Available: Tables of atomic coordinates, bond distances, bond angles, anisotropic thermal parameters, and crystal refinement data for $[\text{Au}_2(\mu\text{-PP}_3)_2]\text{Cl}_2$ and $\text{Au}_4\text{Cl}_4(\mu\text{-PP}_3)$ (19 pages); listings of observed and calculated structure factors (58 pages). Ordering information is given on any current masthead page.

Contribution from the Instituto de Ciencia de Materiales de Madrid, CSIC, Serrano 113, E-28006 Madrid, Spain, and Institut Laue Langevin, BP 156 X, F-38042 Grenoble, France

Tristrontium Dialuminum Hexaoxide: An Intricate Superstructure of Perovskite

J. A. Alonso,^{†,‡} I. Rasines,^{*†} and J. L. Soubeyroux[§]

Received January 5, 1990

$\text{Sr}_3\text{Al}_2\text{O}_6$, obtained as a white powder by solid-state reaction between SrCO_3 and Al_2O_3 , has been studied by X-ray and neutron diffraction. It is cubic, $a = 15.8425(2)$ Å, space group $Pa\bar{3}$, and $Z = 24$. Its crystal structure, refined from the neutron powder data on the basis of the $\text{Ca}_3\text{Al}_2\text{O}_6$ structural model, is described as a superstructure of the perovskites, ABO_3 . Several features, such as oxygen and A deficiency and 1:3 B-cation ordering, which are present simultaneously, suggest that the formula must be rewritten as $\text{Sr}_{7/8}\square_{1/8}(\text{Sr}_{1/4}\text{Al}_{3/4})\text{O}_{9/4}\square_{3/4}$. Bond-valence values obtained for Sr atoms in the A and B subcells are discussed.

Introduction

The structure and composition of tricalcium dialuminum hexaoxide and related compounds are of considerable interest, since $\text{Ca}_3\text{Al}_2\text{O}_6$ (abbreviated to C_3A in cement chemistry), in an impure form, is one of the main components of Portland cement. This compound is cubic, $a = 15.263$ Å, space group $Pa\bar{3}$, and $Z = 24$. The structure¹ consists of rings of six AlO_4 tetrahedra (Al_6O_{18}), eight to a unit cell, surrounding holes of radius 1.47 Å, at $1/8$, $1/8$, $1/8$ and its symmetry-related positions, with Ca^{2+} ions holding the rings together.

$\text{Sr}_3\text{Al}_2\text{O}_6$ is isostructural with C_3A , as indicated by Lagerqvist et al. in an earlier work.² On the other hand, Büsssem and Eitel³ pointed out the similarity of the X-ray powder diffraction patterns of the Sr compound and that of perovskite (CaTiO_3 , $a \approx 3.8$ Å). However, the possible relationship between these structures was not subsequently shown.

The ideal perovskite structure ABO_3 can be briefly described in terms of a cubic unit cell with $a_0 \approx 4$ Å, the smaller B cations being at the corners, the oxygens at the midpoints of the edges, and the larger A cations at the center of the cube. Deficient perovskites, in which A atoms and/or oxygens are partially lacking are well-known.⁴ On the other hand, when the B sites are occupied by two different cations, an ordered arrangement between them is to be expected if their sizes or charges are different enough. A large number of perovskites showing 1:1, 1:2, and 1:3 B-cation ordering, with stoichiometries $\text{A}(\text{B}'_{1/2}\text{B}''_{1/2})\text{O}_3$, $\text{A}(\text{B}'_{1/3}\text{B}''_{2/3})\text{O}_3$, and $\text{A}(\text{B}'_{1/4}\text{B}''_{3/4})\text{O}_3$, respectively, have been described.^{4,5} All these are superstructures of the perovskite, built up with two or more perovskite units and with unit cell parameters related to a_0 .

The aim of this work is to report the crystal structure of $\text{Sr}_3\text{Al}_2\text{O}_6$ and to describe it as a superstructure of perovskite, in which several features (i.e. oxygen and A deficiency and B-cation ordering) are present simultaneously.

Experimental Section

Sample Preparation. $\text{Sr}_3\text{Al}_2\text{O}_6$ has been prepared as a white powder from a stoichiometric mixture of analytical grade SrCO_3 and Al_2O_3 . The sample was ground and heated in air several times, in alumina crucibles, at increasing temperatures between 1073 and 1273 K, for 20 h each, and annealed at 1473 K for 10 h, in order to improve its crystallinity. After each thermal treatment the product was characterized by X-ray diffraction. Total weight losses corresponded to all CO_2 of the starting mixture.

Table I. General Parameters of the Two-Phase Rietveld Refinement

	$\text{Sr}_3\text{Al}_2\text{O}_6$	SrO
space group	$Pa\bar{3}$	$Fm\bar{3}m$
unit cell a param, Å	15.8425 (2)	5.1666 (3)
scale factor	0.00719 (5)	0.137 (7)
vol fraction	97.7 (7)	2.3 (1)
no. of reflcns	1218	15
Bragg R_I factor, %	5.46	4.26
Bragg R_F factor, %	3.29	1.92
profile R_p factor, %	5.30	
profile R_{wp} factor, %	6.88	
expected R_E factor, %	4.14	
no. of observns	2730	
no. of variables	63	

X-ray and Neutron Diffraction. The X-ray powder diffraction pattern was obtained in a Siemens Kristalloflex 810 generator, $\text{Cu K}\alpha$ radiation ($\lambda = 1.540598$ Å), and D500 goniometer, by step-scanning from 10 to 154° in 2θ , in increments of 0.01° in 2θ and with a counting time of 1 s each step. Powdered W, $a = 3.16524(4)$ Å, was used as an internal standard.

The neutron powder diffraction data were collected in the high-resolution D2B⁶ diffractometer at the ILL/Grenoble. The high-intensity mode was used to collect the spectrum, at 295 K. The wavelength, $\lambda = 1.594(1)$ Å, was selected by the 533 planes of a germanium monochromator. The sample was enclosed in a vanadium can of 8-mm diameter and 40-mm height. The 64 counters, spaced at 2.5° intervals, were moved by steps of 0.05° in the range $8^\circ \leq 2\theta \leq 147.5^\circ$.

The neutron diffraction pattern was analyzed by the Rietveld⁷ method, using the Young and Wiles⁸ profile refinement program. A pseudo-Voigt function was chosen to generate the line shape of the diffraction peaks. The coherent scattering lengths for Sr, Al, and O were 7.070, 3.449, and 5.805 fm, respectively.⁹

No regions were excluded in the refinement. Since the presence of small amounts of SrO (with rock-salt structure) was detected in the pattern, the profile refinement of the mixture was performed.

- (1) Mondal, P.; Jeffery, J. W. *Acta Crystallogr., Sect. B* 1975, B31, 689.
- (2) Lagerqvist, K.; Wallmark, S.; Westgren, A. *Z. Anorg. Allg. Chem.* 1937, 234, 1.
- (3) Büsssem, W.; Eitel, A. *Z. Kristallogr. Mineral.* 1936, 95, 175.
- (4) Nomura, S. *Landolt-Börnstein Zahlenwerte und Funktionen aus Naturwissenschaften und Technik. Neue Series*; Springer Verlag: Berlin, 1978; Gruppe III, Band 12a, p 368.
- (5) Alonso, J. A.; Mzayek, E.; Rasines, I. *Mater. Res. Bull.* 1987, 22, 69.
- (6) Hewat, A. W. *Mater. Sci. Forum* 1986, 9, 69.
- (7) Rietveld, H. M. *J. Appl. Crystallogr.* 1969, 2, 65.
- (8) Young, R. A.; Wiles, D. B. *J. Appl. Crystallogr.* 1982, 15, 430.
- (9) Koester, L.; Rauch, H.; Herkens, M.; Schröder, K. Report No. 1975; Kernforschungsanlage: Jülich, FRG, 1981.

[†] Instituto de Ciencia de Materiales de Madrid.

[‡] Present address: Centre d'Etudes Nucléaires de Grenoble, DRF/SPh-MDN, 85X, F-38041 Grenoble, France.

[§] Institut Laue Langevin.

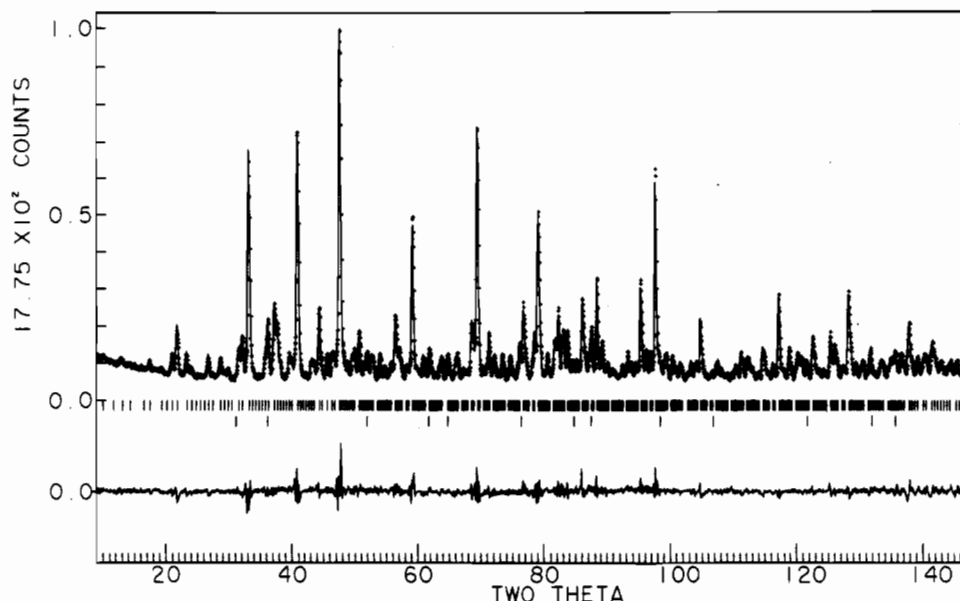


Figure 1. Powder neutron diffraction profile at 295 K. Crosses are the raw data points; the solid line is the best fit profile. The difference plot (observed - calculated) appears at the bottom. The two series of tick marks below the profile indicate the positions of all the allowed reflections included in the calculation, for the phases $\text{Sr}_3\text{Al}_2\text{O}_6$ (1218 reflections) and SrO (15 reflections).

Table II. Structural Parameters for $\text{Sr}_3\text{Al}_2\text{O}_6$, with Esd's in Parentheses

atom	site	x/a	y/b	z/c	$B, \text{\AA}^2$
Sr(1)	4(a)	0	0	0	1.51 (24)
Sr(2)	4(b)	0.5	0	0	1.11 (23)
Sr(3)	8(c)	0.2521 (3)	0.2521 (3)	0.2521 (3)	0.45 (16)
Sr(4)	8(c)	0.3765 (4)	0.3765 (4)	0.3765 (4)	1.13 (12)
Sr(5)	24(d)	0.1345 (3)	0.3745 (3)	0.1332 (4)	0.94 (7)
Sr(6)	24(d)	0.3793 (4)	0.3852 (3)	0.1242 (3)	0.67 (7)
Al(1)	24(d)	0.2520 (5)	0.0164 (8)	0.0184 (8)	0.83 (15)
Al(2)	24(d)	0.2392 (7)	0.2345 (7)	0.0041 (6)	0.70 (17)
O(1)	24(d)	0.2631 (4)	0.1257 (7)	0.0032 (4)	0.93 (10)
O(2)	24(d)	0.4930 (4)	0.1275 (6)	0.2448 (4)	0.79 (9)
O(3)	24(d)	0.2697 (4)	0.2762 (4)	0.1001 (4)	0.96 (10)
O(4)	24(d)	0.2352 (4)	0.4065 (3)	0.2804 (4)	0.79 (11)
O(5)	24(d)	0.3458 (4)	-0.0261 (4)	-0.0188 (5)	1.07 (12)
O(6)	24(d)	0.1544 (4)	-0.0175 (4)	-0.0177 (4)	0.85 (10)

Sixty-three parameters were refined, including six background coefficients; zeropoint; half-width, pseudo-Voigt, and asymmetry parameters for the peak shape; an independent scale factor for $\text{Sr}_3\text{Al}_2\text{O}_6$ and SrO ; positional, thermal isotropic, and unit cell parameters for $\text{Sr}_3\text{Al}_2\text{O}_6$; and thermal overall and unit cell parameters for SrO . The largest observed shift to error value was $\Delta/\sigma = 0.06$.

Results

X-ray Diffraction. The X-ray powder diffraction pattern of $\text{Sr}_3\text{Al}_2\text{O}_6$ corresponds to a cubic compound showing systematic absences ($h00, h = 2n + 1; 0kl, k = 2n + 1$) compatible with the space group $Pa\bar{3}$ (No. 205). The unit cell parameter, $a = 15.8425$ (2) \AA , measured with regard to W peaks, is consistent with the value given by the NBS,¹⁰ $a = 15.844$ (4) \AA . The pattern showed reflections with intensity ratios characteristic of a perovskite-like compound, with $a = 4a_0$ (a_0 being the lattice parameter of the ideal perovskite unit). The strongest superstructure lines ($h + k + l = 4n, h, k, l = 2n$) could be indexed on the basis of a body-centered cubic pseudocell with $a' = a/2$, but the presence of a second series of weaker superlattice reflections ($I/I_0 \leq 4.0$, excepting the reflection 321 with $I/I_0 = 6.9$) made necessary a doubled unit cell.

Neutron Powder Diffraction. The refinement of the neutron pattern according to the structural model described¹ for C_3A led to the final parameters shown in Tables I and II. Bonding

Table III. Main Bonding Distances (\AA) and Angles (deg) for $\text{Sr}_3\text{Al}_2\text{O}_6^a$

B-Cation Polyhedra			
Sr(1)-O(6)	2.479 (6) \times 6	O(6)-Sr(1)-O(6) ⁱ	102.1 (4)
		O(6)-Sr(1)-O(6) ^{vii}	77.9 (3)
Sr(2)-O(5)	2.496 (6) \times 6	O(5)-Sr(2)-O(5) ⁱⁱⁱ	93.7 (3)
		O(5)-Sr(2)-O(5) ^{viii}	86.3 (4)
Sr(3)-O(3)	2.455 (8) \times 3	O(3)-Sr(3)-O(3) ⁱ	104.3 (5)
Sr(3)-O(4)	2.502 (7) \times 3	O(3)-Sr(3)-O(4)	92.1 (4)
		O(3)-Sr(3)-O(4) ⁱ	162.9 (10)
		O(4)-Sr(3)-O(4) ⁱ	87.1 (3)
		O(3)-Sr(3)-O(4) ⁱⁱ	75.9 (3)
Al(1)-O(1)	1.758 (17)	O(1)-Al(1)-O(2) ^{viii}	109.7 (10)
Al(1)-O(2) ^{viii}	1.769 (14)	O(1)-Al(1)-O(5)	104.5 (10)
Al(1)-O(5)	1.735 (12)	O(1)-Al(1)-O(6)	110.4 (10)
Al(1)-O(6)	1.734 (11)	O(2) ^{viii} -Al(1)-O(5)	103.1 (9)
		O(2) ^{viii} -Al(1)-O(6)	106.4 (9)
		O(5)-Al(1)-O(6)	122.1 (10)
Al(2)-O(1)	1.765 (16)	O(1)-Al(2)-O(2) ^{xii}	112.7 (10)
Al(2)-O(2) ^{xii}	1.809 (13)	O(1)-Al(2)-O(3)	108.7 (10)
Al(2)-O(3)	1.728 (12)	O(1)-Al(2)-O(4) ^{ix}	100.5 (9)
Al(2)-O(4) ^{ix}	1.746 (12)	O(2) ^{xii} -Al(2)-O(3)	106.9 (9)
		O(2) ^{xii} -Al(2)-O(4) ^{ix}	103.3 (8)
		O(3)-Al(2)-O(4) ^{ix}	124.8 (10)
A-Cation Polyhedra			
Sr(4)-O(1) ^{vi}	2.695 (11) \times 3	Sr(5)-O(5) ^v	2.897 (10)
Sr(4)-O(4)	2.750 (9) \times 3	Sr(5)-O(5) ^{vi}	2.436 (8)
Sr(4)-O(5) ^{vi}	2.934 (9) \times 3	Sr(6)-O(1) ^{xi}	2.889 (10)
Sr(5)-O(1) ⁱ	2.729 (10)	Sr(6)-O(2) ⁱ	2.732 (10)
Sr(5)-O(2) ⁱ	2.570 (10)	Sr(6)-O(3)	2.479 (9)
Sr(5)-O(2) ^{xii}	2.917 (10)	Sr(6)-O(4) ⁱⁱ	2.457 (7)
Sr(5)-O(3)	2.699 (8)	Sr(6)-O(6) ^v	2.779 (8)
Sr(5)-O(3) ⁱ	2.860 (9)	Sr(6)-O(6) ⁱⁱⁱ	2.433 (8)
Sr(5)-O(4)	2.872 (9)	Sr(6)-O(6) ^{xi}	2.719 (9)

^aSymmetry transformations: (none) x, y, z ; (i) x, z, y ; (ii) y, z, z ; (iii) $1/2 + z, 1/2 - x, -y$; (iv) $-y, 1/2 + z, 1/2 - x$; (v) $1/2 - x, 1/2 + y, z$; (vi) $x, 1/2 - y, 1/2 + z$; (vii) $-z, -x, -y$; (viii) $1/2 - z, 1/2 + x, y$; (ix) $z, 1/2 - x, 1/2 + y$; (x) $1/2 + z, x, 1/2 - y$; (xi) $1/2 - y, 1/2 + z, x$; (xii) $y, 1/2 - z, 1/2 + x$.

distances and angles for the polyhedra around the metallic atoms are listed in Table III. The lattice parameter obtained in the neutron refinement, $a = 15.8476$ (2) \AA , differs slightly from that obtained from the X-ray patterns, indicated above. The difference between these values is, however, within the error expected from the esd of the neutron wavelength, $\pm 0.001 \text{\AA}$.

The agreement between the observed and calculated profiles of the data is shown in Figure 1. Final profile R factors R_p and

(10) NBS Monogr. (U.S.) 1972, 25, 52 (Sect. 10).

(11) Fisher, R. X. *J. Appl. Crystallogr.* 1985, 18, 258.

(12) Johnson, C. K. Report ORNL-3794; Oak Ridge National Laboratory; Oak Ridge, TN, 1965.

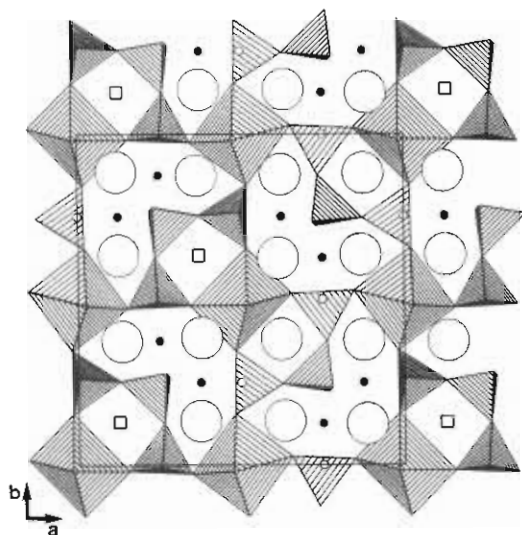


Figure 2. STRUPL011 projection along [001] of the first layer of polyhedra of $\text{Sr}_{7/8}\square_{1/8}(\text{Sr}_{1/4}\text{Al}_{3/4})\text{O}_{9/4}\square_{3/4}$. Octahedra correspond to the Sr(B) atoms, and tetrahedra to the Al atoms, both placed at $z \approx 0$. Large open circles represent Sr(A) atoms, and squares are the vacant sites in the A sublattice, both at $z \approx 1/8$. Small open and solid circles represent oxygen vacancies, at $z \approx 0$ and $z \approx 1/8$, respectively.

R_{wp} , defined in ref 8, were 5.30 and 6.88, respectively; R factors for the integrated intensity and structure factors of the main phase, $\text{Sr}_3\text{Al}_2\text{O}_6$, R_I and R_F , were 5.46 and 3.29, respectively, for 1218 reflections. The expected R factor, $R_E = [(N - P + C) / \sum w_i^2(\text{obs})]^{1/2}$, where $N - P + C =$ number of observations - number of variables + number of constraints, was 4.14. From the refined scale factors of both phases, a volume ratio $\text{SrO} : \text{Sr}_3\text{Al}_2\text{O}_6 = 0.023:1$ was calculated for the sample.

Discussion

Relationship to Perovskite. As far as metallic atoms are concerned, the structure of $\text{Sr}_3\text{Al}_2\text{O}_6$ can be related to that of the perovskites, ABO_3 . From this point of view the formula should be rewritten as $\text{Sr}_{7/8}\square_{1/8}(\text{Sr}_{1/4}\text{Al}_{3/4})\text{O}_{9/4}\square_{3/4}$. In this model, the strontium atoms (Sr(1), Sr(2), Sr(3)), together with Al(1) and Al(2), constitute the B subcell, and Sr(4), Sr(5), and Sr(6) form the A subcell in ABO_3 . Both kinds of Sr atoms are designated hereafter as Sr(B) and Sr(A), respectively. In the whole unit cell there are 64 $\text{Sr}_{7/8}(\text{Sr}_{1/4}\text{Al}_{3/4})\text{O}_{9/4}$ perovskite units, which means 72 Sr, 48 Al, and 144 O atoms.

According to this picture, the perovskite superstructure shows the following features:

1. The oxygen vacancies (48 per unit cell) are ordered in such a way that all the Sr(B) atoms are coordinated to 6 oxygens, keeping the octahedral coordination characteristic of the perovskite structure, whereas all the Al atoms are coordinated to 4 oxygens. The oxygen vacancies are placed at $1/4, 0, 3/8, 3/8, 0, 1/4$, and their symmetry-related positions. Figure 2 corresponds to a c -axis projection of the first layer of polyhedra, in which the ordered disposition of oxygen vacancies is shown. On the other hand, oxygen atoms are shifted from the ideal perovskite positions in order to provide an approximate tetrahedral environment around aluminum atoms, which are also slightly shifted. Figure 3 shows the atomic shifts corresponding to the Al(1) tetrahedron.

2. In the A-cation sublattice one-eighth part (eight per unit cell) of the Sr atoms are lacking. These vacancies are ordered, placed at $1/8, 1/8, 1/8$ and its symmetry-related positions, as shown in Figure 2.

3. In the B subcell Sr(B) and Al atoms are ordered according to a tridimensional arrangement, in which each octant of the unit cell is body centered. This arrangement is in the origin of the strong superstructure reflections with $h + k + l = 4n$ and $h, k, l = 2n$ observed in the X-ray diffraction pattern, due to the large difference in the X-ray scattering factors for Sr and Al. Figure 4 corresponds to an octant of the unit cell, in which the ordered tridimensional arrangement between octahedra and tetrahedra

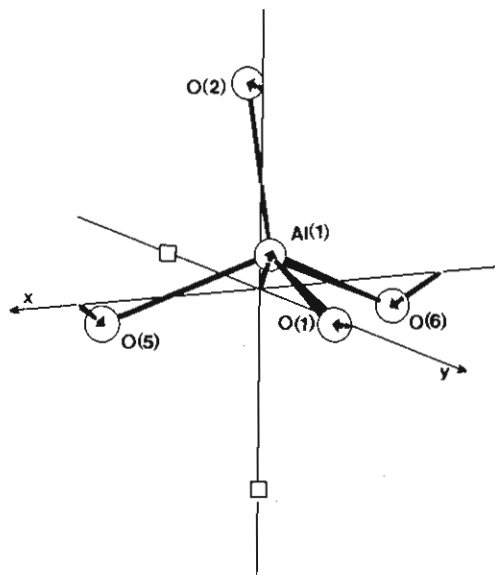


Figure 3. ORTEP¹² picture, showing the oxygen coordination of Al(1) in $\text{Sr}_3\text{Al}_2\text{O}_6$. A tetrahedral environment (fairly irregular) around Al is achieved by means of small shifts of the five atoms from the octahedral positions expected for an ideal perovskite. Shifts for Al(1), O(1), O(2), O(5), and O(6) are 0.21, 0.19, 0.16, 0.65, and 0.61 Å, respectively. The two missing oxygen atoms are represented by squares.

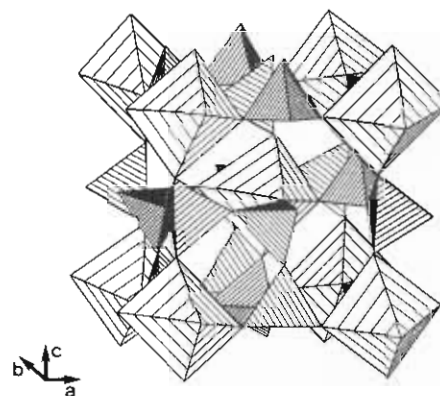


Figure 4. One octant of the unit cell of $\text{Sr}_3\text{Al}_2\text{O}_6$. Octahedra and tetrahedra correspond to $\text{Sr}(\text{B})\text{O}_6$ and AlO_4 , respectively. For the sake of clarity, Sr(A) atoms are not included.

is shown. Octahedral $\text{Sr}(\text{B})\text{O}_6$ groups occupy the vertices and the center of the cube, whereas tetrahedra are placed in the center of the faces and the midpoint of the edges.

Coordination Polyhedra. The Al tetrahedra are rather distorted; Al-O distances and O-Al-O angles are respectively in the range 1.73–1.77 Å and 103.1 – 122.1° for Al(1) and 1.73–1.81 Å and 100.5 – 124.8° for Al(2). Sr(1), as well as Sr(2), is coordinated to six oxygens of one type, forming a distorted octahedron compressed along the 3-fold axis. The polyhedron around Sr(3) (3 O(3) + 3 O(4)) also on the 3-fold axis, is better described as a distorted trigonal prism.

As for the Sr(A) atoms, they occupy rather irregular environments constituted by nine, eight, and seven oxygen atoms for Sr(4), Sr(5), and Sr(6), respectively, at distances ranging between 2.43 and 2.93 Å.

Al_6O_{18} Rings. As in $\text{Ca}_3\text{Al}_2\text{O}_6$,¹ the AlO_4 tetrahedra of $\text{Sr}_3\text{Al}_2\text{O}_6$ share corners to give 6-fold puckered Al_6O_{18} rings centered on 3-fold axes. There are eight such rings surrounding each of the eight vacant A sites of the unit cell. The six Al atoms of each ring occupy six of the vertices of a cube of edge $a_0 \approx 3.96$ Å. The remaining two vertices, on 3-fold axes, are occupied by Sr(B). Figure 5 shows the disposition of one such ring. The hole inside the ring has an effective radius of 1.52 Å, assuming an ionic radius of 1.40 Å for the surrounding O atoms. With respect to the 3-fold axis, the apices of the tetrahedra are alternately pointing in one

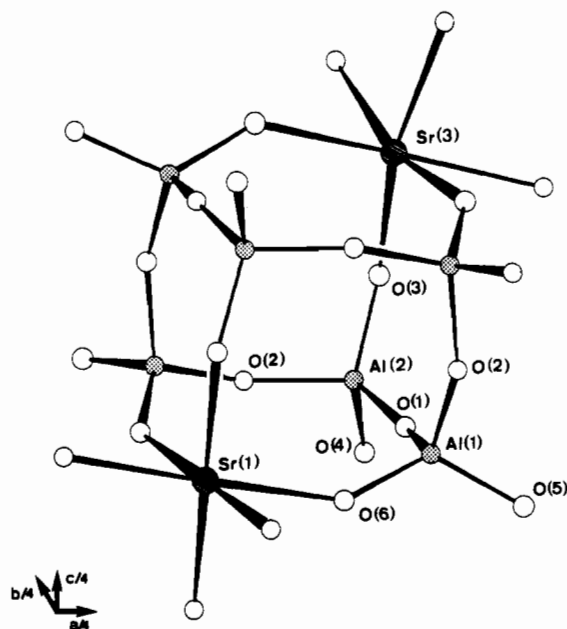


Figure 5. ORTEP¹¹ projection, showing a Al_6O_{18} pucker ring, in chair conformation. This picture can be described as a distorted cube with edge length $\approx a/4$ in which two opposite corners are occupied by Sr(B) atoms and the other six corners by Al, linked together by bridging oxygens. The ring is symmetrical with respect to a 3-fold axis containing both Sr atoms. The center of the cube is empty. Octahedral coordination for Sr(1) and Sr(3) is also shown.

direction and the other. The configuration of the ring may be regarded as a version of the unit ring, in chair conformation, of the tridymite structure.¹³ Al_6O_{18} rings also exist, more or less distorted, in other related compounds such as orthorhombic $\text{Ca}_{8.5}\text{NaAl}_6\text{O}_{18}$.¹⁴

Covalent Framework. With regard to the B-subcell atoms, the tridimensional structure of $\text{Sr}_3\text{Al}_2\text{O}_6$ is built up by octahedra and tetrahedra sharing vertices, in such a way that each octahedron is linked to six tetrahedra and each tetrahedron shares corners with two octahedra and two tetrahedra. The holes between the polyhedra of this framework are occupied by Sr(A) atoms in an ordered way.

Many oxides are constituted of polyhedra BO_n sharing corners, forming a "covalent framework" in which B atoms are strongly bonded to oxygens, whereas the metallic A atoms filling the holes (in general more electropositive) are more weakly bonded. A common feature of these networks is a nonstoichiometry in A. The lack of some A atoms affects the overall stability of the structure very slightly. A very well-known example of BO_6 octahedra sharing corners is that of the pyrochlore structure¹⁵ $\text{A}_2\text{B}_2\text{O}_6\text{O}'$ in which A and O' atoms, weakly bonded, are often partially lacking; the extreme composition, AB_2O_6 , also has the pyrochlore structure.

In $\text{Sr}_{7/8}(\text{Sr}_{1/4}\text{Al}_{3/4})\text{O}_{9/4}$ the same element, Sr, occupies both A and B sites. The bond-valence theory¹⁶ gives an interesting

approach that allows an appreciation in a semiquantitative way of the differences in the chemical environments of both sites.

The values of the valences for all the metallic atoms in the asymmetric unit have been calculated as sums of the valences associated to the bonds listed in Table III. For each individual bond the valence S_i is calculated as $S_i = \exp[(r_0 - r_i)/0.37]$, where $r_0(\text{Al}) = 1.651$, $r_0(\text{Sr}) = 2.118$, and the total valence v of a metallic atom is $v = \sum_i S_i$.

B atoms:	Al(1)	Al(2)	Sr(1)	Sr(2)	Sr(3)
valences:	3.071	3.012	2.265	2.270	2.270
A atoms:	Sr(4)	Sr(5)	Sr(6)		
valences:	1.506	1.621	1.883		

The calculated values for Al atoms are in excellent agreement with those expected. For Sr atoms the valences are systematically higher than 2 for those occupying the B subcell and smaller for those placed at the A-type sites. That means strong, short covalent bonds with oxygen for Sr(1), Sr(2), and Sr(3) and weaker, longer bonds for Sr(4), Sr(5), and Sr(6), with a higher proportion of ionic character. This suggests a mechanism of charge compensation via common oxygens: the valence of the oxygens is almost fully satisfied with the bonding to the B atoms, in such a way that the oxygen-A atom interactions are expected to be predominantly electrostatic. The irregular environment observed for these atoms also suggests the existence of nondirected bonds.

As a consequence of the weak A-O interactions, the absence of some Sr(A) atoms from the structure is not surprising. The ratio of Sr(A) vacancies, one-eighth of the theoretical positions, is that needed to maintain the electroneutrality for the particular stoichiometry $\text{Sr}_3\text{Al}_2\text{O}_6$. Although a precise structure determination has not yet been performed, the structure without A vacancies may exist in the case of the compound $\text{Na}_4\text{CaSi}_3\text{O}_9$, which shows¹⁷ the same powder diffraction pattern, cell size, and space group as those for C_3A .¹ The formula of this silicate could be written on the perovskite key as $\text{Na}(\text{Ca}_{1/4}\text{Si}_{3/4})\text{O}_{9/4}$. In this case the covalent framework should be made of CaO_6 octahedra and SiO_4 tetrahedra sharing vertices, with Na atoms occupying all the A-subcell positions.

The opposite situation, i.e. a structure with the same overall framework and a larger number of A vacancies, could probably be achieved by replacing some of the A or B atoms by cations with similar size and higher charge, i.e. replacing, in $\text{Sr}_3\text{Al}_2\text{O}_6$, Al^{3+} by Si^{4+} and/or Sr cations by lanthanoid cations. Hence, this structural type shows the ability to accommodate certain amounts of cations with different charges without essential changes in the framework, giving rise to nonstoichiometric compounds, through a vacancy mechanism. This suggests that these oxides are, for instance, suitable host lattices for rare-earth-metal cations for optical applications.

Acknowledgment. We thank Dr. C. Cascales for preparing the sample and the ILL for making all facilities available. J.A.A. and I.R. acknowledge the financial aid of the Consejo Superior de Investigaciones Científicas.

Registry No. $\text{Sr}_3\text{Al}_2\text{O}_6$, 12004-40-9; Al_2O_3 , 1344-28-1; SrCO_3 , 1633-05-2; SrO , 1314-11-0.

(13) Wells, A. F. *Structural Inorganic Chemistry*, 5th ed.; Clarendon Press: Oxford, England, 1984; p 1007.

(14) Nishi, F.; Takéuchi, Y. *Acta Crystallogr., Sect. B* **1975**, *B31*, 1169.

(15) Subramanian, M. A.; Aravamudan, G.; Subba Rao, G. V. *Prog. Solid State Chem.* **1983**, *15*, 55.

(16) Brown, I. D.; Altermatt, D. *Acta Crystallogr., Sect. B* **1985**, *B41*, 244.

(17) Maki, I.; Sugimura, T. *Yogyo Kyokai Shi* **1970**, *78*, 23.